Intermittent Chaos in Nonlinear Wave-Wave Interactions in Space Plasmas

Rodrigo A. Miranda,[a,b,1] Erico L. Rempel,[a]
Abraham C.-L. Chian,[a] and Felix A. Borotto[c]

[a] *National Institute for Space Research (INPE) and World Institute for Space Environment Research (WISER), P. O. Box 515, São José dos Campos-SP, 12227-010, Brazil*
[b] *Centro de Estudios del Cuaternario (CEQua), Universidad de Magallanes, Punta Arenas, Chile*
[c] *Departamento de Física, Universidad de Concepción, Concepción, Chile*

Abstract

There is increasing observational evidence of nonlinear wave-wave interactions in space and astrophysical plasmas. We first review a number of theoretical models of nonlinear wave-wave interactions which our group has developed in past years. We next describe a nonlinear three-mode truncated model of Alfvén waves, involving resonant interactions of one linearly unstable mode and two linearly damped modes. We construct a bifurcation diagram for this three-wave model and investigate the phenomenon of intermittent chaos. The theoretical results presented in this paper can improve our understanding of intermittent time series frequently observed in space and astrophysical plasmas.

Keywords: Nonlinear wave-wave interactions; Alfvén waves; intermittency; nonlinear dynamics; chaos

PACS: 52.35.Mw; 52.35.Bj; 05.45.-a

1. Introduction

A number of theoretical models of nonlinear wave-wave interactions have been developed in past years by our group, with several applications to space and astrophysical plasmas. Chian and Kennel (1983) showed that the nonlinearities arising in a model for strong electromagnetic waves propagating in an electron-positron plasma may excite the modulational instability of pulsar radiation, resulting in periodic wave trains or solitons which may account for the formation of pulsar microstructures. Langmuir waves can interact with low-frequency density fluctuations to produce radiations near the local electron plasma frequency, as observed in the upstream of planetary bow shocks and heliopause (Chian, 1990). In the presence of supersonic Langmuir turbulence, electromagnetic radiation near the local electron plasma frequency can be emitted through the electromagnetic parametric instabilities driven by intense Langmuir waves in active experiments in space (Chian, 1991). Standing Alfvén waves can generate convective or purely growing MHD parametric processes in planetary magnetospheres, and large density fluctuations and cavities may result from the ponderomotive interaction of Alfvén and acoustic waves in planetary magnetospheres (Chian and Oliveira, 1994). In Chian and Abalde (1995) a nonlinear analysis of three-wave processes for electrostatic and electromagnetic Langmuir decay processes was performed to interpret observations of highly structured Langmuir wave packets with low-frequency modulations in the interplanetary medium and planetary foreshocks. In Lopes and Chian (1996) a coherent nonlinear theory of three-wave coupling involving Langmuir, Alfvén and whistler waves was formulated and applied to the observation of auroral LAW (Langmuir - Alfvén - Whistler) events in the planetary magnetosphere. Chian et al. (1997) showed that narrow-band circularly polarized ra-

[1] Corresponding author.
Email address: rmiranda@dge.inpe.br (Rodrigo A. Miranda)

dio bursts from the Sun and flare stars can be produced via nonlinear conversion of Langmuir waves into high-frequency electromagnetic electron cyclotron waves by coupling to low-frequency electromagnetic cyclotron waves. Pulsar eclipse due to induced three-wave interactions involving low-frequency acoustic turbulence was discussed in Luo and Chian (1997). Type-III solar radio bursts can be produced by the nonlinear conversion of a traveling Langmuir pump wave into an electromagnetic wave via the coupling of two wave triplets, with the Langmuir pump wave and an ion-acoustic daughter wave common to both wave triplets (Abalde et al., 1998). Abalde et al. (2000) presented a nonlinear three-wave theory describing the parametric interaction of Langmuir, whistler, and circularly polarized electromagnetic waves, in order to account for the observations of close correlations between Langmuir and whistler waves within magnetic holes of the solar wind. In Voitenko et al. (2003) a new nonlinear excitation mechanism of kinetic Alfvén waves and whistler waves in the solar corona via nonlinear coupling with pump Langmuir waves was presented.

In the present work we conduct a study on intermittent chaos in a nonlinear three-wave model of large-amplitude Alfvén waves, obtained as a three-mode truncation of the derivative nonlinear Schrödinger (DNLS) equation in the limit of approximately equal wavelengths among the coupled modes, where one mode is linearly unstable and two modes are linearly damped. We construct the bifurcation diagram in terms of a control parameter representing the damping rate of the linearly damped modes divided by the pump wave growth rate. Two dynamical transitions are discussed. The type-I Pomeau-Manneville intermittency route to chaos (Pomeau and Manneville, 1980), where a stable periodic wave gives rise to a chaotic wave due to its coalescence with an unstable periodic wave as the control parameter reaches a critical value where a saddle-node bifurcation occurs, and the interior crisis transition (Grebogi et al., 1983), where a weakly chaotic wave becomes strongly chaotic. Both types of transition display intermittent time series, where phases of low variabilities are randomly interrupted by phases of very high variabilities. The theoretical results presented in this paper can improve our understanding of intermittent time series frequently observed in space and astrophysical plasmas.

2. Derivative Nonlinear Schrödinger Equation

The dynamics of a large-amplitude nonlinear Alfvén wave propagating along the ambient magnetic field in the x-direction, including linear kinetic effects, is governed by the following form of the DNLS equation (Ghosh and Papadopoulos, 1987):

$$i\left(\frac{\partial}{\partial t}-\hat{\gamma}\right)B+iS_{NL}\frac{\partial}{\partial x}\left(B\left|B\right|^{2}\right)+S_{DIS}\frac{\partial^{2}}{\partial x^{2}}B=0 \tag{1}$$

where $\hat{\gamma}$ is a linear growth/damping operator defined such that the Fourier transform of $\hat{\gamma}$ is $\gamma(k)$, the linear growth or damping as calculated from kinetic theory, S_{NL} is the sign of the nonlinearity, S_{DIS} is the sign of the dispersion, and B is the complex transverse magnetic field.

We consider the following approximate solution of three traveling waves

$$B(x,t)=\sum_{\sigma=0}^{2}B_{\sigma}(t)e^{-i(k_{\sigma}x-\omega_{\sigma}t)} \tag{2}$$

Introducing (2) in (1), and assuming the resonance condition $2k_0=k_1+k_2$, the linear dispersion $\omega_\sigma=-S_{DIS}k_\sigma^2$ ($\sigma=0,1,2$) and the phase difference $\omega_{1,2}-\omega_0\equiv\Delta_{1,2}$, leads to a set of ordinary differential equations for the complex variables B_σ, where we can introduce the following amplitude-phase variables

$$B_{\sigma}(t)\equiv A_{\sigma}(t)exp\left[iX_{\sigma}(t)\right],\quad \sigma=0,1,2 \tag{3}$$

with A_σ and X_σ real. If we assume $A_1=A_2$, $\gamma_1=\gamma_2$, $k_0\approx k_1\approx k_2$, $S_{DIS}=S_{NL}=-1$, and adopt the substitutions

$$\begin{array}{lll}\xi=\gamma_0 t, & a_0^2=(k_0/\gamma_0)A_0^2, & a_1^2=(k_0/\gamma_0)A_1^2\\ \theta=-\psi, & \delta=-\Delta/\gamma_0, & \gamma=-\gamma_1/\gamma_0\end{array}$$

where $\Delta=(\Delta_1+\Delta_2)/2$ and $\psi(t)=2X_0-X_1-X_2-2\Delta t$, then the following set of ODE's is obtained (Russel and Ott, 1981; Ghosh and Papadopoulos, 1987)

$$\dot{a_0} = a_0 + 2a_0a_1^2\sin\theta \quad (4)$$
$$\dot{a_1} = -\gamma a_1 - a_0^2 a_1 \sin\theta \quad (5)$$
$$\dot{\theta} = -2\delta + 2(a_1^2 - a_0^2) + 2(2a_1^2 - a_0^2)\cos\theta \quad (6)$$

where $(\dot{}) \equiv d/d\xi$. The damping rate γ is positive, so that wave 0 is linearly unstable and waves 1 and 2 are linearly damped. Note that an equation for $\dot{a_2}$ is not included in (4)–(6), since we set $a_1 = a_2$ and the expressions for $\dot{a_1}$ and $\dot{a_2}$ are equivalent.

3. Nonlinear Dynamics Analysis

The dynamics of the system (4)–(6) can be studied with the aid of a bifurcation diagram, constructed by choosing one control parameter from the set of equations and varying it, while keeping all other parameters fixed. For each value of the control parameter, equations (4)–(6) are numerically integrated. We fix $\delta = -6$ and choose γ as our control parameter. From the solutions obtained for each value of γ, we ignore the initial transient and plot the points where the flow or *orbit* of (4)–(6) intersects the plane defined by $a_1 = 1$ with $\dot{a_1} < 0$ (i. e. everytime the orbit intersects the plane from "right" to "left"). The points obtained in this way are referred to as Poincaré points. Figure 1(a) shows a periodic window of the bifurcation diagram, and Fig. 1(b) shows the values of the maximum Lyapunov exponent λ_{max} corresponding to each value of γ. Chaos occurs when $\lambda_{max} > 0$, and periodic behavior occurs when $\lambda_{max} < 0$. At $\gamma = \gamma_{SN} \approx 6.7547$, a period-3 stable periodic orbit is created in a *saddle-node bifurcation*, marked SN in Fig. 1. As γ decreases, the periodic orbit evolves from a period-3 to a period-6 orbit, then to a period-12 orbit, and so on. Eventually, this cascade of inverse period-doubling bifurcations leads to a three-band weak chaotic attractor. At $\gamma = \gamma_{IC} \approx 6.7469$ an abrupt enlargement of the chaotic attractor occurs in an event known as *interior crisis* (Grebogi et al., 1983), marked IC in Fig. 1.

When we take a value of γ slightly larger than γ_{SN}, the time series exhibits nearly periodic laminar phases that are randomly interrupted by strong chaotic bursts. This kind of intermittency is known as type-I Pomeau-Manneville intermittency (Pomeau and Manneville, 1981). An example is shown in the Fig. 2(a) for $\gamma = 6.7548$, while Fig. 2(b) shows the corresponding Poincaré points. Figure 2(c) shows the power spectrum for the time series in 2(a) in log-log scale. The broad-band power-law spectrum of Fig. 2(c) is a signature of chaotic motion.

Figure 3 shows the occurrence of the type-I Pomeau-Manneville intermittency in times series represented by Poincaré points near the transition regions of the saddle-node bifurcation. Figure 3(a) shows a period-3 stable periodic orbit for $\gamma = 6.7547$, right after the saddle-node bifurcation point ($\gamma < \gamma_{SN}$). Figure 3(b) shows an intermittent time series where chaotic bursts interrupt the laminar behavior for $\gamma = 6.7548$, just before the bifurcation point ($\gamma > \gamma_{SN}$). Fig. 3(c) shows strong chaos for $\gamma = 6.755$, further away from the bifurcation point.

Figure 4 shows the power spectra in log-linear scale and the phase-space trajectories for a given time interval and two values of γ used in Fig. 3. In Fig. 4(a), the power spectrum consists of discrete peaks, corresponding to a periodic solution (in this case, a period-3 attractor) whose limit cycle is shown in Fig. 4(c). In Fig. 4(b), the power spectrum becomes broad-band and continuous but the peaks of Fig. 4(a) are still recognizable, since between two chaotic bursts the wave displays approximately periodic behavior, as shown in Fig. 3(b). The phase space trajectory shown in Fig. 4(d) reflects the onset of chaos at $\gamma = 6.7548$.

Another type of intermittency occurs at the interior crisis indicated in Fig. 1. The crisis-induced intermittency is characterized by time series containing laminar phases of weak chaotic fluctuations randomly interrupted by strong chaotic bursts (Grebogi et al., 1983; Chian et al., 1998). Figure 5 shows time series (represented by Poincaré points) and phase space trajectories illustrating this crisis-induced intermittency. At $\gamma = 6.7469$, before the interior crisis ($\gamma > \gamma_{IC}$), the time series show no strong chaotic bursts (Fig. 5(a)), and the trajectory is confined to the region of phase space corresponding to the weak chaotic attractor (Fig. 5(d)). At $\gamma = 6.7468$, right after crisis, occasional chaotic bursts appear in the time series, and the trajectory temporarily "escapes" from the region of the weak chaotic attractor (Figs. 5(b) and 5(e)). Strong chaotic bursts become more frequent in the time se-

ries at $\gamma = 6.7467$, further away from crisis, and the trajectory rapidly fills a wider region of the phase-space (Figs. 5(c) and 5(f)).

4. Concluding Remarks

Solar wind observations of Alfvénic fluctuations frequently display erratic and intermittent events (Marsch and Liu, 1993; Bruno et al., 2003) so that an in-depth study of intermittency is essential to understand turbulence in space plasmas. We have presented two mechanisms whereby a three-wave Alfvén system can evolve into chaos and intermittency, namely, type-I Pomeau-Manneville intermittency and interior crisis-induced intermittency. The intermittent time series display broad-band power spectra with a power-law decay of high-frequencies (Fig. 2(c)), a feature similar to the power spectra of MHD turbulence in the solar wind (Marsch and Liu, 1993). The three-mode truncation of the DNLS equation employed in this work imposes limitations on the applicability of the model to interpret fully developed plasma turbulence, where a large number of modes become unstable. The choice of one pump wave and one pair of daughter waves might be justified in the case of weak instabilities, if other sets of daughter waves are strongly damped. However, this model may be useful in a qualitative way in more general situations, since it describes the nonlinear saturation of an unstable mode, and the dynamical behaviors found (e.g., local bifurcations, crisis, intermittent-chaos) are ubiquitous in nonlinear systems.

Acknowledgments

This work is supported by CAPES, FAPESP and CNPq.

References

Abalde, J.R., Alves, M.V., Chian, A.C.-L., 1998. Nonlinear generation of type III solar radio bursts by the hybrid modulational instability. Astronomy and Astrophysics 331 (2), L21–L24.

Abalde, J.R., Borotto, F.A., Chian, A.C.-L., 2000. Generation of circularly polarized radio waves within magnetic holes of the solar wind. Physica A 283 (1-2), 237–242.

Bruno, R., Carbone, V., Sorriso-Valvo, L., Bavassano, B., 2003. Radial evolution of solar wind intermittency in the inner heliosphere. Journal of Geophysical Research 108, 1130.

Chian, A.C.-L., Kennel, C.F., 1983. Self-modulational formation of pulsar microstructures. Astrophysics and Space Science 97, 9–18.

Chian, A.C.-L., 1990. Nonthermal radiation processes in interplanetary plasmas. Revista Mexicana de Astronomia y Astrofisica 21 (SI), 541–544.

Chian, A. C.-L., 1991. Electromagnetic radiation emitted by supersonic Langmuir turbulence in active experiments in space. Planetary and Space Science 39 (8), 1217-1222.

Chian, A.C.-L., Oliveira L.P., 1994. Magneto-hydrodynamic parametric instabilities driven by a standing Alfvén wave in the planetary magneto-sphere. Astronomy and Astrophysics 286 (1), L1–L4.

Chian, A.C.-L., Abalde. J.R., 1995. Nonlinear modulation of Langmuir waves by ion-acoustic-waves in the interplanetary medium and planetary foreshocks, Astronomy and Astrophysics 298 (1), L9–L12.

Chian, A.C.-L., Abalde. J.R., Alves, M.V., Lopes, S.R., 1997. Coherent generation of narrow-band circularly polarized radio bursts from the Sun and flare stars. Solar Physics 173 (1), 199–202.

Chian, A.C.-L., Borotto, F.A., Gonzalez, W.D., 1998. Alfvén intermittent turbulence driven by temporal chaos. Astrophysical Journal 505 (2), 993–998.

Ghosh, S., Papadopoulos, K., 1987. The Onset of Alfvénic Turbulence. Physics of Fluids 30 (5), 1371–1387.

Grebogi, C., Ott, E., Yorke, J.A., 1983. Crises, sudden changes in chaotic attractors, and transient chaos. Physica D 7, 181–200.

Lopes, S.R., Chian, A.C.-L., 1996. A coherent nonlinear theory of auroral Langmuir-Alfvén-Whistler (LAW) events in the planetary magneto-sphere. Astronomy and Astrophysics 305 (2), 669–676.

Luo, Q.H., Chian, A.C.-L., 1997. Pulsar eclips-

ing mechanisms: the effect of photon-beam-induced acoustic turbulence. Monthly Notices of the Royal Astronomical Society 289 (1), 52–58.

Marsch, E., Liu, S., 1993. Structure functions and intermittency of velocity fluctuations in the inner solar-wind. Annales Geophysicae 11, 227–238.

Pomeau, Y., Manneville, P., 1980. Intermittent transition to turbulence in dissipative dynamical systems. Communications in Mathematical Physics 74, 189–197.

Russell, D. A., Ott, E., 1981. Chaotic (strange) and periodic behavior in instability saturation by the oscillating two-stream instability. Physics of Fluids 24 (11), 1976-1988.

Voitenko, Y., Goossens, M., Sirenko, O., Chian, A.C.-L., 2003. Nonlinear excitation of kinetic Alfvén waves and whistler waves by electron beam-driven Langmuir waves in the solar corona. Astronomy and Astrophysics 409 (1) 331–345.

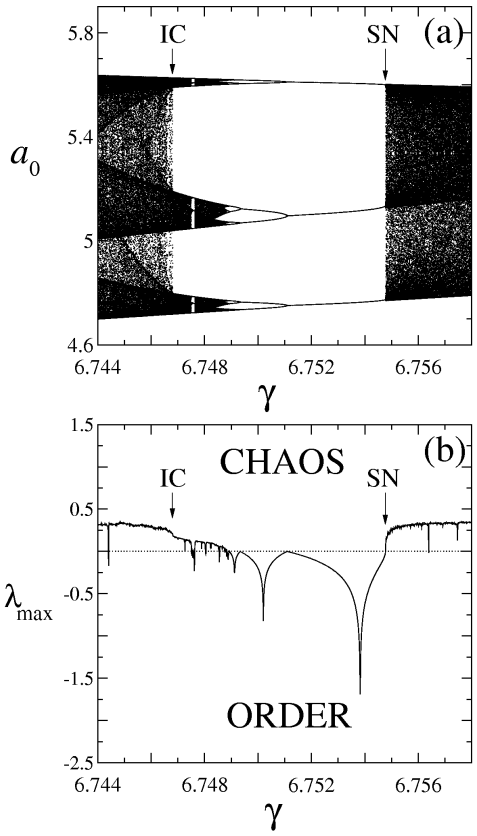

Figure 1: (a) Bifurcation diagram for a_0 as a function of the decay wave damping rate γ for a period-3 window; SN denotes *saddle-node bifurcation* and IC denotes *interior crisis*; (b) maximum Lyapunov exponent λ_{max} as a function of γ.

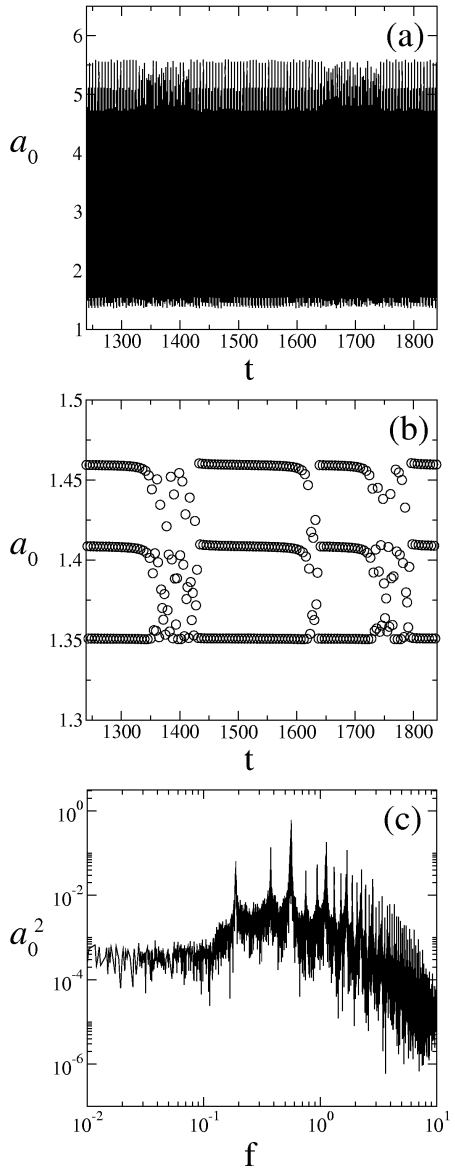

Figure 2: (a) Example of type-I Pomeau-Manneville intermittent chaos at $\gamma = 6.7548$; (b) the same time series of (a) represented by Poincaré points; (c) power spectrum of the time series in (a) in log-log scale.

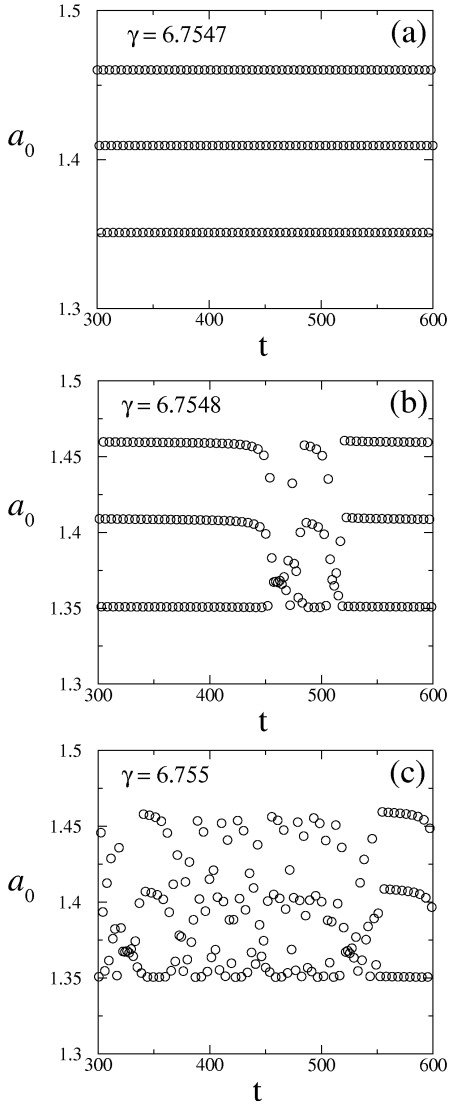

Figure 3: Time series of a_0 for the type-I Pomeau-Manneville intermittency route to chaos for (a) $\gamma = 6.7547$, (b) $\gamma = 6.7548$, and (c) $\gamma = 6.755$.

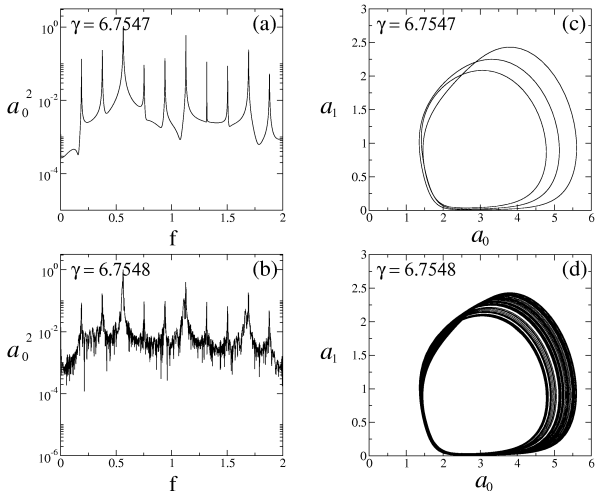

Figure 4: Power spectra in log-normal scale for (a) $\gamma = 6.7547$ and (b) $\gamma = 6.7548$ with the corresponding trajectories in the phase space (a_0, a_1) in (c) and (d).

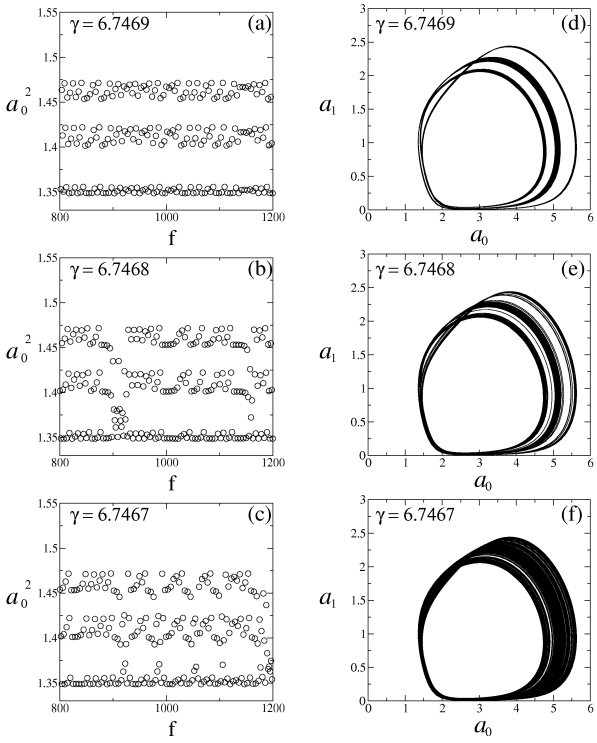

Figure 5: Time series of a_0 for the crisis-induced intermittency for (a) $\gamma = 6.7469$, (b) $\gamma = 6.7468$ and (c) $\gamma = 6.7467$, with the corresponding trajectories in the phase space (a_0, a_1) in (d) to (f).